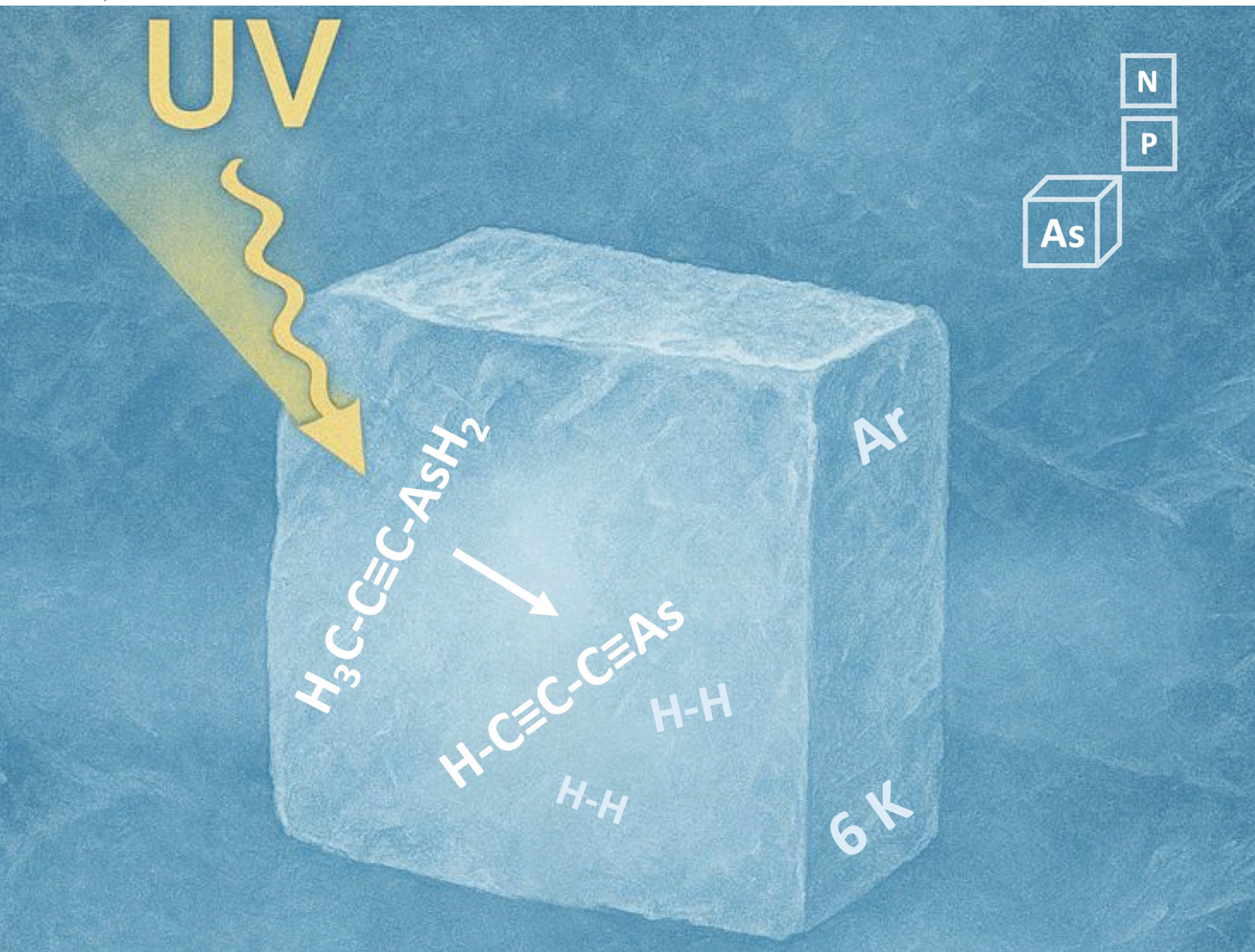


# Dalton Transactions

An international journal of inorganic chemistry

rsc.li/dalton



ISSN 1477-9226

Cite this: *Dalton Trans.*, 2026, **55**, 1642Received 19th November 2025,  
Accepted 9th December 2025

DOI: 10.1039/d5dt02772a

rsc.li/dalton

## HC<sub>3</sub>As, the simplest arsadiyne

Arun-Libertsen Lawzer,<sup>a</sup> Thomas Custer,<sup>a</sup> Jean-Claude Guillemin<sup>b</sup> and Robert Kotos<sup>a</sup>

**1-Arsabutadiyne (2-propynylidynarsine, HC<sub>3</sub>As), is efficiently produced by photolysis of propynylarsine isolated in solid argon. The observed infrared absorption spectra and predicted molecular parameters of HC<sub>3</sub>As and HC<sub>3</sub>P show significant similarities, but large differences compared to HC<sub>3</sub>N.**

Cyanoacetylene, HC<sub>3</sub>N, first synthesized over a century ago,<sup>1</sup> has been extensively characterized, partly because of its importance for molecular astrophysics. The molecule has been detected<sup>2–6</sup> in galactic gas clouds, circumstellar envelopes, comets, the atmosphere of Titan, and also in extragalactic locations. It constitutes the first element in the series of rod-like nitriles H-(CC)<sub>*n*</sub>-CN represented in space up to at least *n* = 4.<sup>7,8</sup> Spectroscopic data available for HC<sub>3</sub>P are sparse, limited to the gas-phase rotational (microwave) domain<sup>9</sup> and to the vibrational (infrared) spectrum of the cryogenically isolated molecule.<sup>10</sup> The arsenic analogue of cyanoacetylene is expected to be less stable than HC<sub>3</sub>N and HC<sub>3</sub>P, as it features a mono-coordinated arsenic atom with inherently unfavorable π-bonds between the 4p orbital of arsenic and the 2p orbital of carbon. To the best of our knowledge, no theoretical or experimental studies on HC<sub>3</sub>As have been reported.

Typically, molecules containing the –C≡As moiety are kinetically unstable,<sup>11</sup> therefore laboratory studies of such compounds are rare. Their instability can be overcome by protecting the arsaalkyne centre with bulky substituents and by electron delocalization, as demonstrated for 2-(2,3,6-tri-*tert*-butylphenyl)-1-arsaethyne.<sup>12</sup> The simplest arsaalkyne, HC≡As, has been detected in the gas phase with photoelectron spectroscopy and mass spectrometry.<sup>13</sup> Arsaalkynes CH<sub>3</sub>CAs<sup>14</sup> and CH<sub>3</sub>CH<sub>2</sub>CAs,<sup>15</sup> which exhibit half-lives of less than 30 minutes in room-temperature solutions, have been characterized by NMR spectroscopy with additional infrared and microwave

spectroscopic measurements made only for CH<sub>3</sub>CAs. To the best of our knowledge, no other reports of experimental observation of free arsaalkynes can be found in the literature.

Our previous studies demonstrated that small pnictogen-containing molecules such as HCCPH<sub>2</sub>, HCCAsH<sub>2</sub>, and HCCSbH<sub>2</sub> undergo efficient photodehydrogenation to yield the corresponding radicals: HCCP, HCCAs, and HCCSb, respectively.<sup>16,17</sup> More recently, we reported on photolysis of CH<sub>3</sub>CH<sub>2</sub>CP in a solid argon matrix, where HC<sub>3</sub>P was produced *via* an intermediate species, 1-propynylphosphine.<sup>10</sup> In the present work, we adopt a similar strategy using 1-propynylarsine (CH<sub>3</sub>CCAsH<sub>2</sub>) as a precursor for HC<sub>3</sub>As (Scheme 1).

As propynylarsine is prone to degradation even when stored at –78 °C, it was freshly synthesized prior to each experiment from propynylchloroarsine following the procedure described by Lassalle *et al.*<sup>15</sup> and collected in a glass trap at –196 °C.

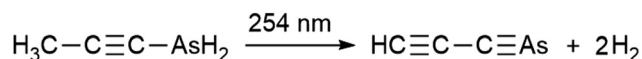
For matrix isolation studies, a mixture of argon and propynylarsine sublimed from the trap (molar ratio 500 : 1) was deposited onto a caesium iodide window maintained at 10 K within a closed-cycle helium cryostat. The main impurities detected in the cryogenic sample were AsH<sub>3</sub> and traces of 1-arsabutyne (CH<sub>3</sub>CH<sub>2</sub>C≡As; an isomer of propynylarsine).

A detailed description of this experimental setup and the applied quantum chemical methods is provided in the SI.

IR absorption features produced by photolyzing (Hg lamp, 254 nm) the precursor molecules isolated in cryogenic argon matrices are compared in Fig. 1 with anharmonic frequencies and IR absorption band intensities computed at the coupled cluster level of theory. A set of easily discernible, mutually correlated photoproduct bands developed upon UV irradiation. Based on theory, they are unambiguously attributed to 1-arsabutadiyne (Fig. 1, 2; Table 1). All bands of this simplest arsadiyne having

<sup>a</sup>Institute of Physical Chemistry, Polish Academy of Sciences, ul. Marcina Kasprzaka 44/52, 01-224 Warsaw, Poland. E-mail: alawzer@ichf.edu.pl, thomas.custer@ichf.edu.pl, rkotos@ichf.edu.pl

<sup>b</sup>Univ Rennes, Ecole Nationale Supérieure de Chimie de Rennes, CNRS, ISCR, UMR6226, F-35000 Rennes, France. E-mail: jean-claude.guillemin@ensc-rennes.fr



Scheme 1 Photochemical generation of 1-arsabutadiyne.



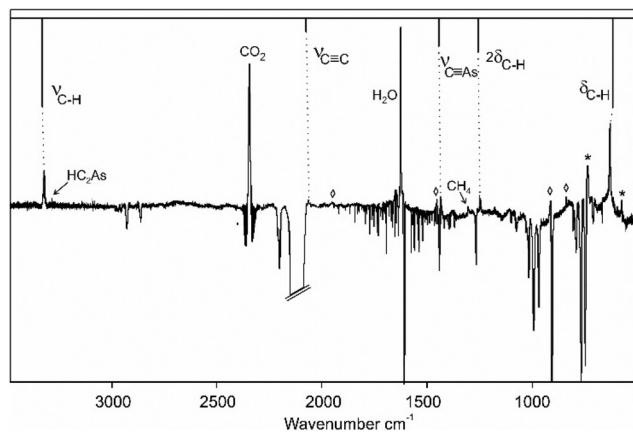


**Fig. 1** Identification of  $\text{HC}_3\text{As}$  via IR absorption. Bottom: difference spectrum showing the net effect of 20 hours of 254 nm photolysis of 1-propynylarsine isolated in solid argon (precursor bands point downwards, product bands point upwards). Top: spectrum predicted at the VPT2/CCSD(T)/aug-cc-pVTZ level of theory. Diamonds mark the bands of tentatively assigned products:  $\text{CH}_2\text{CHCAs}$  and  $\text{CH}_2\text{CCHAsH}_2$  (SI S9 and S5). Asterisks indicate artifact features originating in the irradiated Csl substrate window.

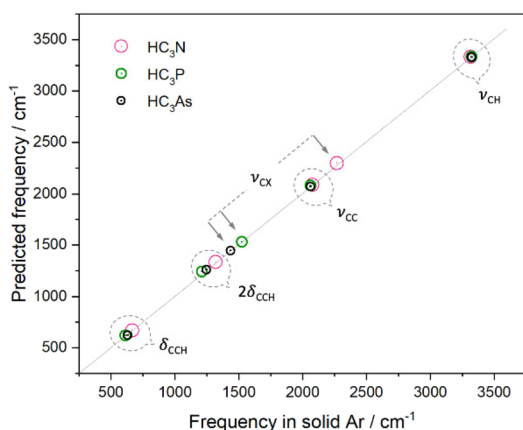


**Fig. 2** Vibrational frequencies observed in solid Ar for  $\text{HC}_3\text{X}$  compounds ( $\text{X} = \text{As}, \text{P}, \text{N}$ ) and theoretically derived (VPT2/CCSD(T)/aug-cc-pVTZ). Points indicated with arrows refer to the  $\text{C}\equiv\text{X}$  stretching mode. See Fig. S1 of SI for graphical representations of the fundamental modes. Experimental data come from ref. 18 ( $\text{HC}_3\text{N}$ ), ref. 10 ( $\text{HC}_3\text{P}$ ), and this work ( $\text{HC}_3\text{As}$ ).

the predicted intensities greater than  $1 \text{ km mol}^{-1}$  and falling in our detection range were observed, including the 1st overtone of  $\delta(\text{CCH})$ . However, accurate determination of the  $\nu_{\text{CAs}}$  frequency in the vicinity of  $1436 \text{ cm}^{-1}$  was hampered by the overlapping methyl group vibration bands of the precursor molecule (SI, S8c). After *ca.* 20 hours of irradiation, the concentration of photoproducted  $\text{HC}_3\text{As}$  reached a plateau and the conversion ratio of propynylarsine to arsabutadiyne could be estimated as 15 to 25 percent, based on theoretically predicted IR band intensities of both compounds (see S4 of SI and Table 1).

Data collected in Fig. 2 and Table 1 allow comparison of the measured IR bands of  $\text{HC}_3\text{As}$  with those of its phos-

phorus-<sup>10</sup> and nitrogen-bearing<sup>18</sup> analogues observed in solid Ar. The measured frequencies of  $\nu_{\text{CH}}$  and  $\nu_{\text{CC}}$  stretching vibrations are practically insensitive to the replacement of arsenic with either phosphorus or nitrogen (see Fig. S1 of SI for a graphical representation of the fundamental modes). More pronounced (*i.e.*, on the order of several percent) are the corresponding changes revealed for the  $\delta_{\text{CCH}}$  mode and its first overtone. There, the frequency does not decrease monotonically from the lightest to the heaviest compound but reaches a minimum for  $\text{HC}_3\text{P}$ . As shown in Table 1 (see also Fig. S2 of SI), this non-trivial effect is reproduced with calculations, provided that the anharmonic approach is applied. The most pronounced influence of pnictogen atom exchange on the IR spectrum is observed in  $\text{HC}_3\text{X}$  molecules ( $\text{X}$  denoting pnictogen) for the  $\nu_{\text{CX}}$  stretching band (Fig. 2; see also Fig. S3 of SI). Compared to cyanoacetylene, the respective frequency is reduced by 33% in  $\text{HC}_3\text{P}$  and 37% in  $\text{HC}_3\text{As}$ , in agreement with the theoretical result (33% and 36%, respectively).

Differences in vibrational frequencies observed for  $\text{HC}_3\text{X}$ -family molecules reflect the varying masses of  $\text{X}$  atoms and electronic charge distributions. Phosphorus and arsenic have similar, low electronegativities, while nitrogen is more electronegative than carbon. Some of the ensuing molecular properties can be traced with natural bond orbital (NBO) analysis. The computed natural atomic charges (Fig. 3) indicate strongly positive values on the phosphorus and arsenic centers, in contrast to the negative charge on nitrogen. This is reflected in CCSD(T)/aug-cc-pVTZ predictions of the equilibrium electric dipole moment: 3.72, 0.75, and 0.43 debyes for  $\text{HC}_3\text{N}$ ,  $\text{HC}_3\text{P}$ , and  $\text{HC}_3\text{As}$ , respectively.

The Wiberg bond indices<sup>19</sup> show a progressive decrease in the carbon–pnictogen bond order from  $\text{HC}_3\text{N}$  to  $\text{HC}_3\text{As}$ , consistent with the expected weakening of  $\pi$ -interactions.<sup>11</sup>

While some traces of other products, apart from  $\text{HC}_3\text{As}$ , were found in the irradiated sample, it is worth noting that the overall photolysis yield, and hence the number of detectable products, is significantly lower here than in a recently reported<sup>10</sup> study on propynylphosphine in solid Ar. We identified allenylarsine,  $\text{CH}_2\text{CCHAsH}_2$  (based on weak bands at  $838.0 \text{ cm}^{-1}$  and  $1956.2 \text{ cm}^{-1}$ ) (SI S5), just as allenylphosphine was the main product (along with  $\text{HC}_3\text{P}$ ) of propynylphosphine photolysis. Similarly, vinylarsaethyne,  $\text{CH}_2\text{CHCAs}$ , was observed (tentatively), analogous to  $\text{CH}_2\text{CHCP}$  obtained<sup>10</sup> by single photodehydrogenation of propynylphosphine. Vinylarsaethyne (SI S9) is a plausible intermediate *en route* to  $\text{HC}_3\text{As}$ .

Traces of HCCAs and methane were also detected upon photolysis. That pair of compounds may arise (by analogy with the photochemistry of propynylphosphine) through decomposition of a transiently formed isomer, most likely HCCAs(H)  $\text{CH}_3$ . The characterization of HCCAs and methane was based on their CH stretching<sup>17</sup> and bending bands<sup>20</sup> at  $3284.5 \text{ cm}^{-1}$  and  $1304.5 \text{ cm}^{-1}$  (SI S10).

Arsabutyne ( $\text{CH}_3\text{CH}_2\text{C}\equiv\text{As}$ ), observed as an impurity in the unphotolyzed sample (SI Fig. S6), most likely isomerizes to propynylarsine upon irradiation and further decomposes to  $\text{HC}_3\text{As}$ .



**Table 1** Measured and theoretically derived vibrational wavenumbers ( $\text{cm}^{-1}$ ) of  $\text{HC}_3\text{X}$ s, compared to those reported for  $\text{HC}_3\text{P}$  and  $\text{HC}_3\text{N}$ . Values in parentheses are the theoretical (in  $\text{km mol}^{-1}$ ) and experimental (relative) IR band intensities. X stands for pnictogen. See Fig. S1f or the graphical representation of fundamental vibrations

| Mode <sup>a</sup>             | H-C≡C-C≡As                   |              |                         | H-C≡C-C≡P                    |              |                               | H-C≡C-C≡N                    |               |                         |
|-------------------------------|------------------------------|--------------|-------------------------|------------------------------|--------------|-------------------------------|------------------------------|---------------|-------------------------|
|                               | Theory (CCSD(T)/aug-cc-pVTZ) |              |                         | Theory (CCSD(T)/aug-cc-pVTZ) |              |                               | Theory (CCSD(T)/aug-cc-pVTZ) |               |                         |
|                               | Harmonic                     | VPT2         | Ar matrix               | Harmonic                     | VPT2         | Ar matrix <sup>10</sup>       | Harmonic                     | VPT2          | Ar matrix <sup>18</sup> |
| $\nu(\text{CH})$              | 3436<br>(83)                 | 3328<br>(71) | 3323.4, 3321.1<br>(100) | 3445<br>(79)                 | 3333<br>(68) | 3322.7                        | 3443<br>(71)                 | 3332<br>(64)  | 3314.9, 3315.9          |
| $\nu(\text{CC})$              | 2106<br>(15)                 | 2072<br>(11) | 2062.7<br>(6)           | 2127<br>(18)                 | 2082<br>(12) | 2062.8                        | 2121<br>(2)                  | 2089<br>(1.7) | 2076.5                  |
| $\nu(\text{CX})$              | 1465<br>(21)                 | 1445<br>(23) | 1436 <sup>b</sup>       | 1553<br>(30)                 | 1531<br>(30) | 1524.3                        | 2337<br>(14)                 | 2297<br>(11)  | 2268.7                  |
| $\nu(\text{CCX})$             | 567<br>(1)                   | 563<br>(1)   | Not detected            | 693<br>(0.5)                 | 683<br>(0.1) | Not detected                  | 888<br>(0.2)                 | 873<br>(0.0)  | Not detected            |
| $\delta(\text{CCH})$          | 603<br>(70)                  | 624<br>(73)  | 630.0, 629.0<br>(95)    | 616<br>(69)                  | 621<br>(71)  | 611.2, 611.8,<br>613.1, 614.0 | 675<br>(73)                  | 671<br>(71)   | 665.7, 667.3            |
| $2\delta(\text{CCH})$         | —                            | 1259<br>(31) | 1247.0<br>(14)          | —                            | 1241<br>(27) | 1212.2                        | —                            | 1334<br>(18)  | 1318.3                  |
| $\delta(\text{CCCX})$ zig-zag | 500<br>(2)                   | 513<br>(0.2) | Not detected            | 506<br>(2)                   | 511<br>(1)   | Not detected                  | 548<br>(9)                   | 535<br>(12)   | 502.1, 503.5            |
| $\delta(\text{CCCX})$ banana  | 197<br>(20)                  | 196<br>(18)  | Out of range            | 209<br>(16)                  | 203<br>(15)  | Out of range                  | 237<br>(0.4)                 | 225<br>(0.4)  | 222.4 <sup>c</sup>      |

<sup>a</sup> S2 (SI) provides the graphical representation of all fundamental modes. <sup>b</sup> Estimation of intensity and the determination of exact maxima of the band was hampered by an overlapping propynylarsine band. <sup>c</sup> Gas phase; ref. 21.

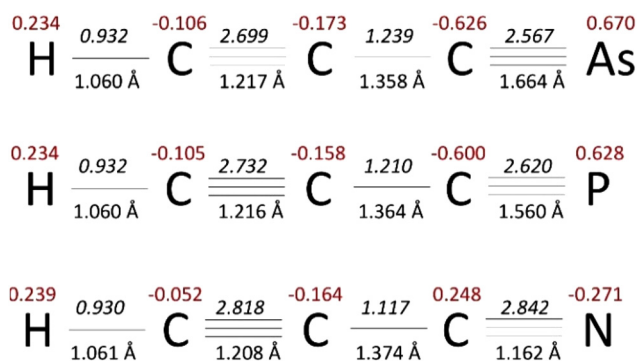


**Fig. 3** CCSD(T)/cc-pVTZ interatomic distances predicted for three  $\text{HC}_3\text{X}$  molecules, together with the select natural bond orbital analysis results: Wiberg bond indices (italics) and natural atomic charges (red).

The identification of  $\text{HC}_3\text{As}$ , the major product of propynylarsine photolysis, opens the way to its further chemical and spectroscopic characterization.

## Conflicts of interest

There are no conflicts to declare.

## Data availability

All data supporting the findings of this study are available within the article and the supplementary information (SI).

Additional raw experimental and computational data are available from the corresponding author upon reasonable request.

Supplementary information is available. See DOI: <https://doi.org/10.1039/d5dt02772a>.

## References

- 1 C. Moureu and J.-C. Bongrand, *C. R. Acad. Sci.*, 1910, **151**, 946.
- 2 B. E. Turner, *Astrophys. J.*, 1971, **163**, L35.
- 3 V. Bujarrabal, M. Guelin, M. Morris and P. Thaddeus, *Astron. Astrophys.*, 1981, **99**, 239.
- 4 D. Bockelée-Morvan, D. C. Lis, J. E. Wink, D. Despois, J. Crovisier, R. Bachiller, D. J. Benford, N. Biver, P. Colom, J. K. Davies, E. Gérard, B. Germain, M. Houde, D. Mehringer, R. Moreno, G. Paubert, T. G. Phillips and H. Rauer, *Astron. Astrophys.*, 2000, **353**, 1101.
- 5 A. Coustenis, B. Bézard, D. Gautier, A. Marten and R. Samuelson, *Icarus*, 1991, **89**, 152.
- 6 J. E. Lindberg, S. Aalto, F. Costagliola, J.-P. Pérez-Beaupuits, R. Monje and S. Muller, *Astron. Astrophys.*, 2011, **527**, A150.
- 7 R. L. Snell, F. P. Schloerb, J. S. Young, A. Hjalmarson and P. Friberg, *Astrophys. J.*, 1981, **244**, 45.
- 8 N. W. Broten, T. Oka, L. W. Avery, J. M. MacLeod and H. Kroto, *Astrophys. J.*, 1978, **223**, L105.
- 9 L. Bizzocchi, C. Degli Esposti and P. Botschwina, *Chem. Phys. Lett.*, 2000, **319**, 411.
- 10 A.-L. Lawzer, E. Ganesan, T. Custer, J.-C. Guillemin and R. Kołos, *Phys. Chem. Chem. Phys.*, 2025, **27**, 7556.



- 11 L. Weber, *Chem. Ber.*, 1996, **129**, 367–379; L. L. Lohr and A. C. Scheiner, *J. Mol. Struct.: THEOCHEM*, 1984, **18**, 195; T. Marino, M. C. Michelini, N. Russo, E. Sicilia and M. Toscano, *Theor. Chem. Acc.*, 2012, **131**, 1141.
- 12 G. Märkl and H. Sejpka, *Angew. Chem., Int. Ed. Engl.*, 1986, **25**, 264, (*Angew. Chem.*, 1986, **98**, 286).
- 13 J.-C. Guillemin, A. Chrostowska, A. Dargelos, T. X. M. Nguyen, A. Graciaa and P. Guenot, *Chem. Commun.*, 2008, 4204.
- 14 J.-C. Guillemin, L. Lassalle, P. Dréan, G. Wlodarczak and J. Demaison, *J. Am. Chem. Soc.*, 1994, **116**, 8930.
- 15 L. Lassalle, S. Legoupy and J.-C. Guillemin, *Inorg. Chem.*, 1995, **34**, 5694.
- 16 A.-L. Lawzer, T. Custer, J.-C. Guillemin and R. Kołos, *Angew. Chem., Int. Ed.*, 2021, **60**, 6400.
- 17 A.-L. Lawzer, E. Ganesan, M. Gronowski, T. Custer, J.-C. Guillemin and R. Kołos, *Chem. – Eur. J.*, 2023, **29**, e202300887.
- 18 F. Borget, T. Chiavassa, A. Allouche, F. Marinelli and J.-P. Aycard, *J. Am. Chem. Soc.*, 2001, **123**, 10668.
- 19 K. B. Wiberg, *Tetrahedron*, 1968, **24**, 1083.
- 20 M. G. Govender and T. A. Ford, *J. Mol. Struct.*, 2000, **550**, 445–454.
- 21 A. Jolly, Y. Benilan and A. Fayt, *J. Mol. Spectrosc.*, 2007, **242**, 46–54.

